INTERNATIONAL JOURNAL of RENEWABLE ENERGY RESEARCH
M. Mokhlis et al., Vol.9, No.2, June, 2019

Robust Control for Photovoltaic System Under Partial Shading Effect Using the SEPIC Converter

Mohcine Mokhlis*‡, Mohammed Fefra*, Ahmed Abbou*, Rafika El idrissi*

* Department of Electrical Engineering, Mohammadia School of Engineers, Mohammed V University, Ibn Sina Street P.B 765, Rabat

(mohcine1mo@gmail.com, mohaferfra@gmail.com, abbou_a@yahoo.fr, rafika.elidrissi@gmail.com)

‡ Corresponding Author; Mohcine Mokhlis, Tel: +212 628 984 358,

mohcine1mo@gmail.com

Received: 01.02.2019 Accepted:15.03.2019

Abstract- Under the partial shading effect, the photovoltaic modules are subjected to the non-uniform insolation. In this case, the Power-Voltage curve contains several maximum power points (global and local maximums). In fact, the MPPT algorithms such as P&O and IC, cannot distinguish the global maximum. Thus, a considerable drop in power is produced. To tackle this problem, this article proposes a SLG-backstepping technique. This latter, sweeps the Power-Voltage curve, looks for the global maximum power point, and generates the reference of optimal voltage. Then, the backstepping control was designed to pursue the reference voltage by adjusting the duty cycle of the SEPIC converter. This algorithm was simulated on MATLAB/SIMULINK environment, evaluated under uniform and non-uniform insolation and compared to the PSO with backstepping control. In this latter, the PSO (Particle Swarm Optimization) serves to generate the voltage reference that corresponds to the Global Maximum Power Point, while the backstepping controller tracks this voltage reference. According to the results, the SLG-backstepping algorithm is accurate and has a fast convergence time is about 40ms until 50ms depends on the shading pattern.

Keywords Backstepping control, Partial Shading Effect, Particle Swarm Optimization, Photovoltaic Panel, SEPIC Converter.

Nomenclature

C_{out}: Output capacitor
C_{PV}: Input capacitor
D: Diode of the SEPIC converter
D_{BP1}, D_{BP2}: Bypass diodes
DC: Direct current
GMPP: Global Maximum Power Point
GMPPT: Global Maximum Power Point Tracking
I_{cell}, V_{cell}: Current and voltage of a photovoltaic cell.
I_{L1}, I_{L2}: The input and filter coil inductances
I_m, V_m: Optimal current and voltage
I_{rr}: Irradiation
K_1, K_2: The control parameters
L_1, L_2: The SEPIC converter coils
MPP: Maximum Power Point
MPPT: Maximum Power Point Tracking
P-V: Power-Voltage
PSO: Particle Swarm Optimization
PV: Photovoltaic
SEPIC: Single Ended Primary Inductor Converter
SLG: Sweep, Look and Generate
T: Temperature
T_1: Transistor of the SEPIC converter
V_i: Step increment of V_{inc}
V_{inc}: Voltage increment
V_{C1}: Filter capacitor voltage
V_{out}: Output voltage
V_r: The voltage that changes from 0 to V_{oc}
V_{ref}: The reference voltage
V_t: Thermal voltage

1. Introduction

Unlike the fossil fuel energies (coal, oil, natural gas, etc.), whose stocks are non-renewable and limited in the human scale, the renewable energy is an inexhaustible, a non-polluting and an unlimited source. In fact, the photovoltaic energy is the most used because it can be installed close to the consumer, which minimizes the cost and the power losses due to the transport of electrical energy.

The energy produced by the photovoltaic panel is not maximal, because the power production depends on the load. To overcome this problem, the power converter is necessary to control the energy to be maximal whatever the load. For this reason, several techniques have been proposed. In fact, Perturb and Observe (P&O) and incremental conductance (IC) [1]-[2] are widely used for their simplicity of implementation. But these algorithms cannot be accurate and fast at the same time [3]. The nonlinear controllers proposed in [4]-[5] accurately track the maximum power point (MPP). However, these controllers cause a considerable drop of power when the partial shading takes place [6].

Under the non-uniform insolation, the power-voltage curve presents several points of local maximum and a single point of global maximum [7]. Knowing that, the MPPT technique cannot distinguish between the local and the global maximum [8]. Therefore, it often causes the power losses. Indeed, under the non-uniform meteorological conditions, the current of the unshaded modules passes through the bypass diodes of the shaded modules to protect them against the hotspot heating [9]. But the bypass diodes create several maximum power points in the P-V curve [10].

In [11], the Perturb, Observe and Check Algorithm (POC) is proposed to improve the P&O algorithm and to make it able to track the global maximum power point (GMPP). However, the P&O algorithm is applied several times to locate all the maximum power points available in the P-V curve. In [12], the author has proposed the OC&P (Observe, Compare, and Perturb) method to improve the POC algorithm. Here, the comparison process was designed to look for the global maximum (desired maximum). Then, the P&O algorithm was applied only one time to oscillate around the desired maximum. The PSO (Particle Swarm Optimization) algorithm [13], is one of the optimization methods that are able to pursue the global maximum. But this algorithm isn't accurate and tracks slowly the desired maximum.

In [14] and [15], two stages were proposed. The measurement stage and the adaptation stage (BOOST converter). In fact, in [14], the measurement stage was controlled to generate the reference of optimal voltage. while, in [15], the measurement stage was controlled to generate the reference of the Global Maximum Power Point. Then, the duty cycle of the second stage was adjusted to track the generated reference. But the measurement stage is not preferable, because it increases the installation cost and complexity.

The DMPPT (Distributed MPPT) and MIC (Module Integrated converter) topologies, which are proposed in [16]-[17]-[18], are more powerful than the methods previously discussed. In fact, these topologies don't require the bypass diodes, and extract the power of each photovoltaic module under uniform and non-uniform weather conditions [18]. But these topologies are expensive and the installation cost depends on the number of installed photovoltaic modules.

In this article, the SLK-backstepping technique is designed to track the GMPP. Here, the SLK is an algorithm which is proposed to look for the optimal voltage. This one corresponds to the global maximum power point. In fact, the algorithm detects any change of insolation. Then, it starts increasing the reference voltage from 0 to V_{oc} by sweeping the P-V curve. Therefore, the algorithm gives the optimal voltage. The backstepping is a nonlinear controller that is designed to track the optimal voltage of the PV panel given by the SLK algorithm, using the DC/DC SEPIC converter. The SLK-backstepping proposed algorithm allows to obtain a photovoltaic system with an accurate tracking of the global maximum and a fast response to any atmospheric changes.

This article is organized as follows: Section 2 presents the proposed system and the photovoltaic panel and the SEPIC converter modelling. In Section 3, the proposed technique is well detailed. Section 4 is devoted to the simulation results. Finally, the last section is dedicated to the conclusion.

2. Proposed System

As shown in Fig. 1, the proposed system consists of a photovoltaic source, a DC/DC converter and a resistive load of 150Ω. In fact, two photovoltaic modules (Reference: Shell SM55) have been connected in series. Table 1. shows the electrical characteristics of Shell SM55 PV module. The maximum power, generated under standard weather conditions (Irradiation of 1000W/m^2 and Temperature of 25°C), is approximately 55W. Thus, the power produced by this photovoltaic source is 110W.

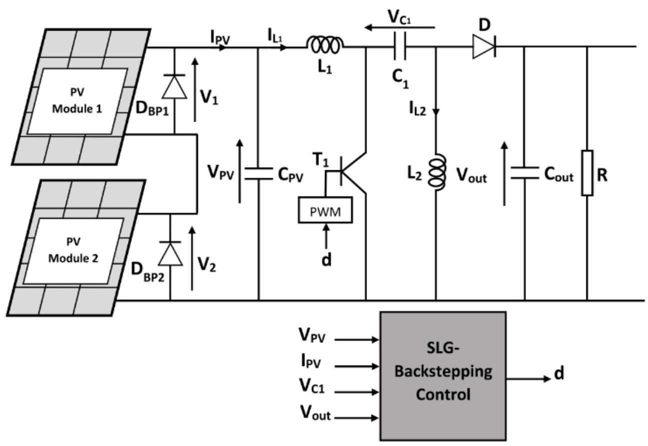

Fig. 1. Proposed photovoltaic system.

Table 1. Electrical characteristics of Shell SM55 PV model

Parameters	Values
Maximum power P_{max}	55W
Optimum voltage V_{opt} for P_{max}	17.4V
Optimum current I_{opt} for P_{max}	3.15A
Maximum current I_{sc} (Short-circuit current)	3.45A
Maximum voltage V_{oc} (open circuit voltage)	21.7V
Temperature coefficient K_i of I_{sc}	1.4×10^{-3}A/°C
Number of cells in series N	36

The SEPIC converter has been used for its many advantages. In reality, against the Buck-Boost converter, this converter makes it possible to have a non-inverted and constant output voltage, and allows to have an input current with weak ripples [19]-[20]. In addition, The SEPIC converter is able to operate from I_{sc} to V_{oc} by changing the duty cycle [19]. Also, it is able to operate in Buck and BOOST mode according to the duty cycle value [21].

The proposed system has been modeled mathematically to obtain the following state equations [21]:

$$\begin{cases} \dot{V}_{PV} = \dfrac{1}{C_{PV}} I_{PV} - \dfrac{1}{C_{PV}} I_{L1} \\ \dot{I}_{L1} = \dfrac{1}{L_1} V_{PV} - \dfrac{1}{L_1}(1-d)(V_{C1} + V_{out}) \\ \dot{V}_{C1} = \dfrac{1}{C_1}(1-d) I_{L1} + d\dfrac{1}{C_1} I_{L2} \\ \dot{I}_{L2} = d\dfrac{1}{L_2} V_{C1} - (1-d)\dfrac{1}{L_2} V_{out} \\ \dot{V}_{out} = \dfrac{1}{C_{out}}(I_{L1}+I_{L2})(1-d) - \dfrac{1}{C_{out}R} V_{out} \end{cases} \quad (1)$$

2.1. Modelling of Photovoltaic Panel

In this study, a single-diode photovoltaic cell was considered, see Fig. 2. The mathematical equation of a photovoltaic module of Ns cells is as follows:

$$I_{PV} = I_{ph} - I_S\left[\exp\left(q\frac{V_{PV} + I_{PV}R_S}{AN_SKT}\right) - 1\right] - \frac{V_{PV} + I_{PV}R_S}{R_P} \quad (2)$$

With I_{ph} is the photo-current, I_S is the saturation current, N_S is the number of photovoltaic module cells, A is the ideality factor, K is the Boltzmann constant ($1.3806503e^{-23}$J/K), T is the cell temperature in Kelvin, q is the electron charge ($1.60217646e^{-19}$C), R_S is the series resistor, R_P is the parallel resistor and V_{PV} and I_{PV} are respectively the photovoltaic panel voltage and current. The mathematical models of the current I_{ph} and I_S are given in [22].

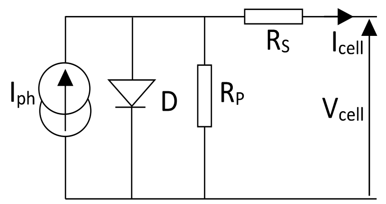

Fig. 2. Single-diode photovoltaic cell.

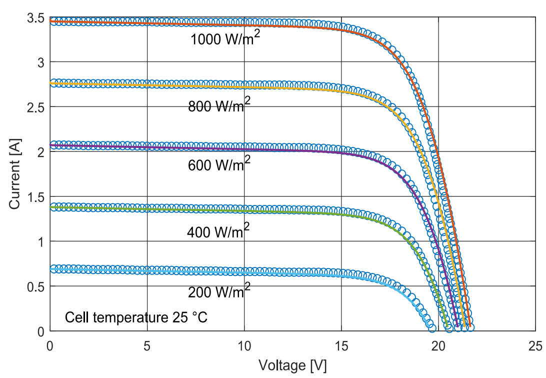

Fig. 3. I–V model curves and experimental data of the Shell SM55 solar module at different irradiation, 25°C.

The photo-current is defined by the expression:

$$I_{ph} = \left[I_{ph0} + K_i(T - T_{STC})\right]\frac{G}{G_{STC}} \quad (3)$$

With G_{STC} and T_{STC} are respectively the irradiation and the temperature at the standard conditions (G_{STC} = 1000W/m^2 and T_{STC} = 25°C), I_{ph0} is the photo-current measured under these conditions, and K_i is the temperature coefficient of I_{SC}.

The saturation-current I_S is written as follows:

$$I_S = I_{S0}\left(\frac{T}{T_{STC}}\right)^3 \exp\left(q\frac{E_G}{AK}\left(\frac{1}{T_{STC}} - \frac{1}{T}\right)\right) \quad (4)$$

With E_G is the band-gap energy ($E_G \approx 1.12$eV for solar cells of polycrystalline silicon) and I_{S0} is the saturation current measured at the nominal temperature $T = T_{STC}$.

As can be seen in equations (2), (3) ad (4), there are five unknown parameters to identify R_S, R_P, A, I_{S0} and I_{ph0}. A is considered equal to 1.3 [23]. Therefore, there remain four parameters to identify, these constants were measured under the standard conditions by using Table 1 and the following expressions as given in [23] and [24]:

$$\begin{cases} I_{ph0} = \left(\dfrac{R_S + R_P}{R_P}\right) I_{SC} \\ I_{S0} = \dfrac{I_{SC}}{\exp\left(\frac{V_{oc}}{V_t}\right) - 1} \\ \exp\left(\dfrac{V_m + R_S I_m - V_{oc}}{V_t}\right) = \dfrac{A}{B - C} \\ R_P = \dfrac{D(V_m - R_S(I_{SC} - I_m) - V_t)}{D(I_{SC} - I_m) - V_t I_m} \end{cases} \quad (5)$$

Where:

$$\begin{cases} V_t = \dfrac{AKN_S T_{STC}}{q} \\ A = V_m V_t(2I_m - I_{SC}) \\ B = D(V_m I_{SC} + V_{oc}(I_m - I_{SC})) \\ C = V_t(V_m I_{SC} - V_{oc} I_m) \\ D = (V_m - I_m R_S) \end{cases} \quad (6)$$

The adjusted parameters are illustrated in Table 2. Fig. 3 and Fig. 4 show the mathematical I-V curve of a PV module (Reference: SHELL SM55) plotted with the experimental data at five levels of temperature and irradiation. As can be seen, the developed PV module fits the electric model behavior to the experimental data. Therefore, the calculated equivalent circuit works properly.

Table 2. Parameters of adjusted Shell SM55 PV model at standard conditions

Parameters	**Values**
Ideality Factor A	1.3
Series resistor R_S	0.3355Ω
Parallel Resistor R_P	235.9Ω
Photo-current I_{ph0}	3.455A
Saturation current I_{S0}	5.013×10^{-8}A

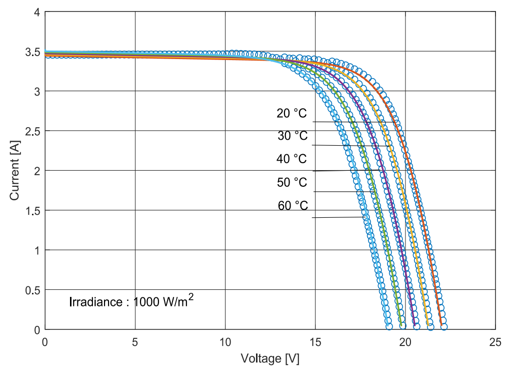

Fig. 4. I–V model curves and experimental data of the Shell SM55 solar module at different temperatures, $1000W/m^2$.

3. Proposed Technique

Under the non-uniform conditions of irradiation and temperature, the P-V curve has several points of maximum power (local and global maximums). The proposed technique serves to locate the global maximum and the corresponding (optimal) voltage. The backstepping is a nonlinear control that is designed to follow the reference voltage by adjusting the duty cycle of the SEPIC converter.

The flowchart, shown in Fig. 5, presents the proposed SLG-backstepping technique. As can be seen, the algorithm begins generating the voltage reference (V_{ref}), this one gradually increases from 0 to V_{oc} and returns the optimal voltage value (V_{opt}). While, the backstepping control follows V_{ref}.

3.1. Sweep interval of the P-V curve

As Fig. 3 and Fig. 4 show, the open circuit voltage V_{oc} is not constant and depends on the insolation. However, the scanning process of the P-V curve must stop if V_{ref} has caught V_{oc}. To solve this problem, the following condition has been proposed:

$$\begin{cases} V_{PV} \geq V_x \\ p_{PV} \leq p_x \end{cases} \quad (7)$$

Where V_x = 17V and P_x = 5W. In fact, as shown in Fig. 6 and Fig. 9, when the condition (7) is true, it defines the voltage nearest to V_{oc}. When this voltage, which called superior voltage V_{sup} is captured, the scan of the P-V curve ends. In the other hand, the inferior voltage V_{inf} was also defined to be 5V instead of zero. Thus, these limits reduce the time of scanning process of the P-V curve.

3.2. Partial Shading Detection

The SLG algorithm repeats the search for the maximum global power point after any change in weather conditions. But to detect the insolation change, one of the following conditions must be fulfilled:

$$\begin{cases} V_{PV} - V_{opt} \leq -\Delta V \\ P_{PV} - P_{max} \leq -\Delta P \end{cases} \quad (8)$$

$$P_{PV} - P_{max} \geq \Delta P \quad (9)$$

With ΔP and ΔV are the partial shading detection thresholds.

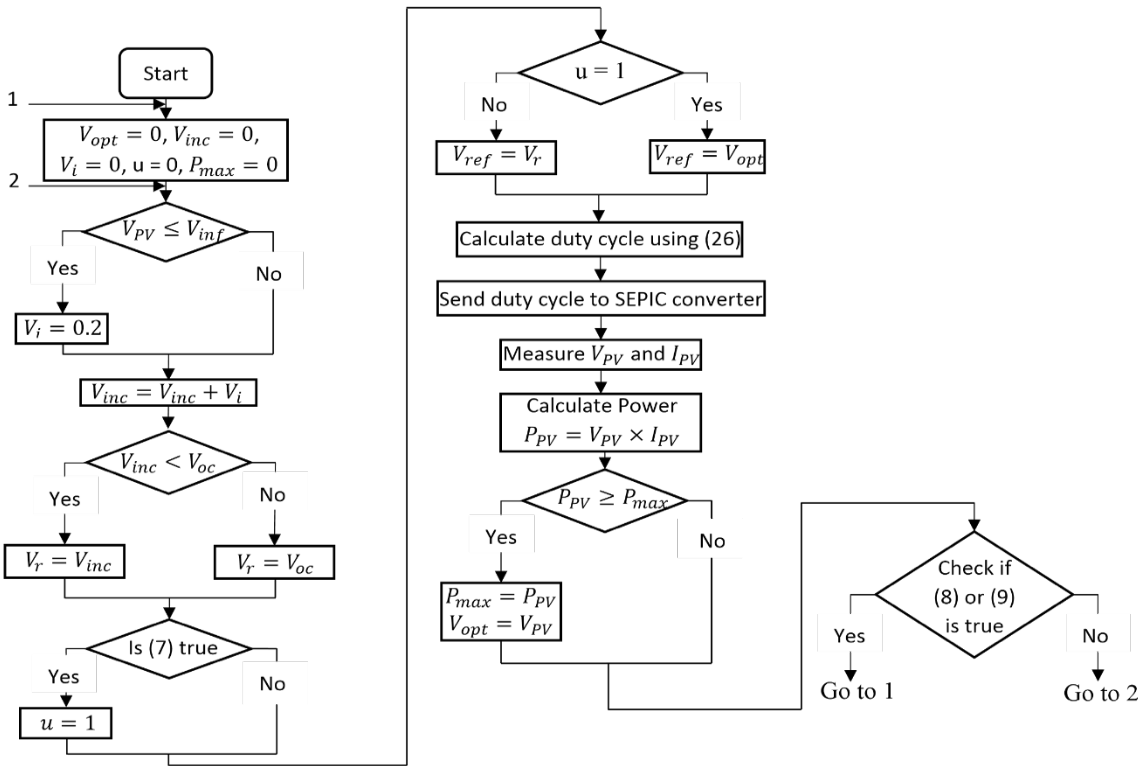

Fig. 5. Flowchart of the SLG-backstepping technique.

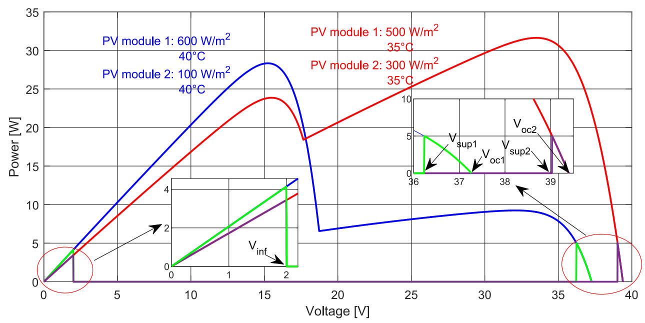

Fig. 6. Sweep interval of the P-V curve.

3.3. Backstepping control

To design the backstepping control, it has to define the output y and the reference y_{ref} to follow. Knowing that, this nonlinear controller is designed to track the reference of optimal voltage. Therefore, y will be the photovoltaic voltage V_{PV}. While, y_{ref} will be the reference voltage V_{ref}.

The steps design of the backstepping control are as follows:

Step 1: define the tracking error ε_1:

$$\varepsilon_1 = y - y_{ref} = V_{PV} - V_{ref} \tag{10}$$

The time derivative of ε_1 gives:

$$\dot{\varepsilon}_1 = \dot{V}_{PV} - \dot{V}_{ref} \tag{11}$$

Thus:

$$\dot{\varepsilon}_1 = \frac{I_{PV} - I_L}{C_{PV}} - \dot{V}_{ref} \tag{12}$$

Then, the following function is applied to ensure the stability:

$$V_1 = \frac{1}{2}{\varepsilon_1}^2 \tag{13}$$

The time derivative of V_1 gives:

$$\dot{V}_1 = \varepsilon_1\dot{\varepsilon}_1 = \varepsilon_1\left(\frac{I_{PV} - I_L}{C_{PV}} - \dot{V}_{ref}\right) \tag{14}$$

The virtual control α_1 = $(I_{L1})_d$ is chosen to allow the stabilization of ε_1. Where $(I_{L1})_d$ is the desired value of inductor current. The virtual control α_1 would be:

$$\frac{I_{PV} - \alpha_1}{C_{PV}} - \dot{V}_{ref} = -K_1\varepsilon_1 < 0 \tag{15}$$

With $K_1 > 0$

Thus, α_1 is as follows:

$$\alpha_1 = -C_{PV}\dot{V}_{ref} + I_{PV} + C_{PV}K_1\varepsilon_1 \tag{16}$$

Step 2:

$$\varepsilon_2 = I_L - \alpha_1 \tag{17}$$

The time derivative of ε_2 is:

$$\dot{\varepsilon}_2 = \frac{1}{L_1}V_{PV} - \frac{1}{L_1}(1-d)(V_{C1} + V_{out}) - \dot{\alpha}_1 \tag{18}$$

Where:

$$\dot{\alpha}_1 = F\dot{V}_{PV} + C_{PV}K_1\dot{\varepsilon}_1 - C_{PV}\ddot{V}_{ref} \tag{19}$$

With:

$$\dot{I}_{PV} = \frac{\partial I_{PV}}{\partial t} = \frac{dI_{PV}}{dV_{PV}}\frac{dV_{PV}}{dt} = F\dot{V}_{PV} \tag{20}$$

And:

$$F = \frac{\partial I_{PV}}{\partial V_{PV}} = -I_S\frac{q}{AN_SKT}\exp\left(q\frac{V_{PV}}{AN_SKT}\right) \tag{21}$$

Here, to simplify calculations, F was calculated considering that the series resistor R_S is negligible while the parallel resistor R_P is infinite.

The Lyapunov function is applied as follows:

$$V_2 = V_1 + \frac{1}{2}{\varepsilon_2}^2 \tag{22}$$

The time derivative would be:

$$\dot{V}_2 = \dot{V}_1 + \varepsilon_2\dot{\varepsilon}_2 \tag{23}$$

Knowing that:

$$\dot{V}_1 = -K_1{\varepsilon_1}^2 - \frac{\varepsilon_1\varepsilon_2}{C_{PV}} \tag{24}$$

Consequently:

$$\dot{V}_2 = -K_1{\varepsilon_1}^2 - \frac{\varepsilon_1\varepsilon_2}{C_{PV}} + \varepsilon_2\dot{\varepsilon}_2 \tag{25}$$

The following condition must satisfied to allow converging ε_2 to zero:

$$-\frac{\varepsilon_1}{C_{PV}} + \dot{\varepsilon}_2 = -K_2\varepsilon_2 < 0 \tag{26}$$

With $K_2 > 0$

So, the real control is:

$$d = \left[L_1\left(-K_2\varepsilon_2 + \frac{\varepsilon_1}{C_{PV}} + \dot{\alpha}_1\right) - V_{PV}\right]\frac{1}{V_{C1} + V_{out}} + 1 \tag{27}$$

Thus:

$$\dot{V}_2 = -K_1{\varepsilon_1}^2 - K_2{\varepsilon_2}^2 < 0 \tag{28}$$

Which ensures $\varepsilon = (\varepsilon_1, \varepsilon_2)$ converges asymptotically to 0. Thus, y converges to y_{ref}.

4. Simulation Result

Two photovoltaic modules (Reference: Shell SM55) have been connected in series and subjected to the different meteorological conditions, as shown in Fig. 7. In fact, as can be seen in this figure, from 0s to 1.13s, the photovoltaic modules were subjected to the uniform insolation level. While, in the range 1.13s ≤ t ≤ 5s, the PV modules have been subjected to the partial shading effect. The used parameters for the photovoltaic system are as follows:

The SEPIC converter parameters:
C_{PV} = 440µF, L_1 = 0.35mF, L_2 = 0.35mF, C_1 = 440µF, C_{out} = 740µF, R = 150Ω.

The SLG-backstepping technique parameters are taken:
V_{inf} = 5V, ΔP = 0.006W, ΔV = 0.006V, K_1 = 437, K_2 = 209.

The PSO-backstepping technique parameters:
w = 0.1, c_1 = 0.2, c_2 = 1, K_1 = 435, K_2 = 500.

Where c_1 and c_2 are the acceleration coefficients, and w is the inertia weight.

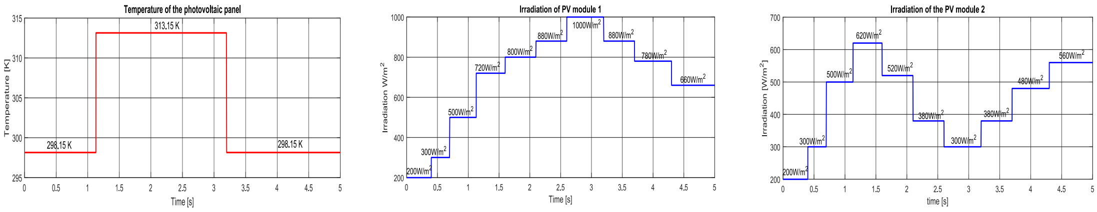

(a) (b) (c)

Fig. 7. Meteorological conditions.

Fig. 8 shows the produced photovoltaic power using SLG and PSO algorithms with the backstepping control. As can be seen, after any change of insolation, the proposed technique follows the global maximum power point more quickly than the PSO-backstepping technique. In fact, the PSO algorithm is widely used, thanks to its simplicity of implementation, lower cost and its ability to follow the global maximum power [26]. But it has a drawback such as the parameter adjusting difficulties [27] and slower convergence time.

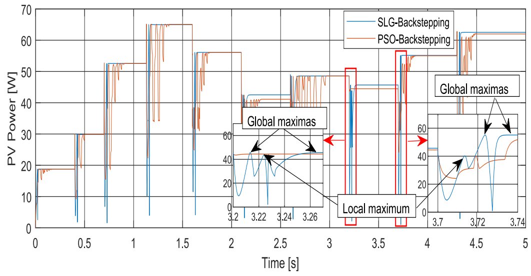

Fig. 8. Photovoltaic power.

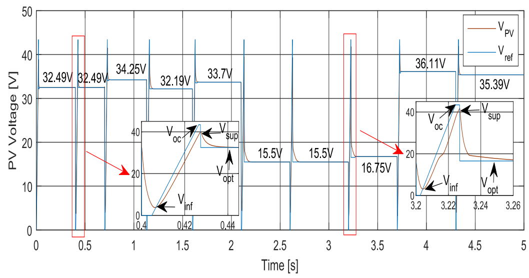

Fig. 9. Photovoltaic voltage.

As Fig. 9 depicts, the reference voltage increases from 0 to V_{oc}, then returns the optimal voltage. In other hand, the photovoltaic voltage (V_{PV}) follows V_{ref} without exceeding the upper and lower limits (V_{inf} and V_{sup}). As can be seen in this figure, the search and tracking time of V_{opt} is about 40ms. But this time depends on the insolation level, in the worst case, the follow-up time does not exceed 50ms.

Fig. 10-a shows the duty cycle of the SEPIC converter. While, Fig. 10-b illustrates the current of the photovoltaic panel. Fig. 11-a, Fig. 11-b and Fig. 11-c respectively depict the current, voltage and power across the load.

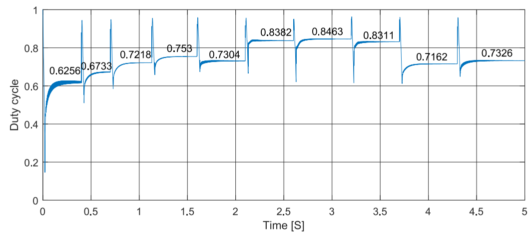

(a)

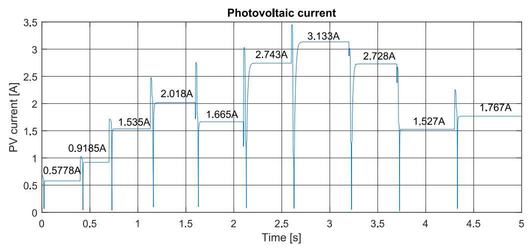

(b)

Fig. 10. (a) Duty cycle, (b) Photovoltaic current.

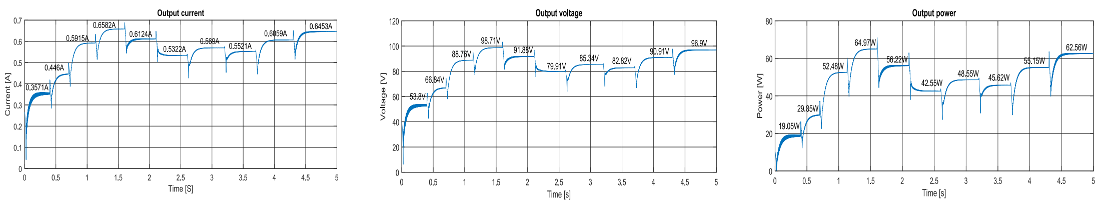

(a) (b) (c)

Fig. 11. Output current, voltage and power.

5. Conclusion

A new technique has been proposed to track the global maximum power point. This one is a combination of SLG algorithm and bakstepping control. The SLG algorithm has been proposed to provide the reference of optimal voltage, that corresponds to the GMPP, whenever the insolation changes. While, the backstepping control has been designed to track the reference voltage by adjusting the duty cycle of the SEPIC converter.

The SLG-backstepping technique was proposed to provide fast and accurate tracking performance and to have a PV system able to locate the global maximum. Knowing that the PSO algorithm can also track the GMPP and return the optimal voltage reference, for this reason, and to show the effectiveness of the proposed algorithm, a comparison between SLG and PSO was made. After testing these two algorithms in MATLAB/SIMULINK environment and associate them with the backstepping control, the results show that the SLG algorithm can track the optimal voltage more quickly than the PSO algorithm. Also, the proposed technique can operate under all environmental conditions.

References

[1] Zaidi Asma, Dahech Karim, Damak Tarak, “Maximum Power Point Tracking of Photovoltaic Systems Based on Fast Terminal Sliding Mode Controller”, International Journal of Renewable Energy Research, Vol.6, No.4, 2016.

[2] Karima Amara, Arezki Fekik, D. Hocine, Mohamed Lamine Hamida, El-Bay Bourennane, Toufik Bakir and Ali Malek, “Improved Performance of a PV Solar Panel with Adaptive Neuro Fuzzy Inference System ANFIS based MPPT”, 7th International Conference on Renewable Energy Research and Applications, Paris, France, pp. 1098 – 1101, Oct. 14-17, 2018.

[3] Kashif Ishaque, Zainal Salam, Muhammad Amjad and Saad Mekhilef, “An Improved Particle Swarm Optimization (PSO)–Based MPPT for PV With Reduced Steady-State Oscillation”, IEEE Transactıons on Power Electronıcs, Vol. 27, No. 8, August 2012, pp. 3627-3638.

[4] M.Guisser, A. EL-Jouni, M. Aboulfatah and E. Abdelmouniim, “Nonlinear MPPT Controller for Photovoltaic Pumping System Baset on Robust Integral Backstepping Approach”, International Review on Modeling and Simulations (I.RE.MOS), Vol. 7, N. 3, ISSN 1974-9821, June 2014.

[5] Saloua Marhraoui, Ahmed Abbou, Abdellah Ziouh, Nezha El hichami, Sallah eddine Rhaili, “Robust Integral Backstepping Approach for MPPT in Different Models of Solar Panel”, 7th International Conference on Renewable Energy Research and Applications, Paris, France, pp. 371 – 376, Oct. 14-17, 2018.

[6] L.Bouselham, M.Hajji, B. Hajji, H.Bouali, “A MPPT-Based ANN Controller Applied To PV Pumping System”, 2016 International Renewable and Sustainable Energy Conference (IRSEC), ISSN 2380-7393, Marrakech, Morocco, pp. 86 - 92, 2016.

[7] C. Sakthigokulrajan and K. Ravi, “Combined role of derived array configurations and MPSO based MPPT in improving the energy yield under partial shading conditions”, Journal of Building Engineering, Vol. 9, January 2017, pp. 125-134.

[8] Kashif Ishaque, Zainal Salam, Hamed Taheri, Syafaruddin, “Combined role of derived array configurations and MPSO based MPPT in improving the energy yield under partial shading conditions”, Simulation Modelling Practice and Theory, Vol. 19, Issue 7, August 2011, pp. 1613-1626.

[9] M. Davarifar, A. Rabhi, A. Hajjaji, E. Kamal and Z. Daneshifar, “Partial shading fault diagnosis in PV system with discrete wavelet transform (DWT)”, 2014 International Conference on Renewable Energy Research and Application, Milwaukee, WI, USA, pp. 810 - 814, 2014.

[10] A. Dolara, S. Leva, G. Magistrati, M. Mussetta, E. Ogliari and R. Varun Arvind, “A novel MPPT algorithm for photovoltie systems under dynamic partial shading - Recurrent scan and track method”, 2016 IEEE International Conference on Renewable Energy Research and Applications (ICRERA), Birmingham, UK, pp. 1122 – 1127, 2016.

[11] R. Alonso, P. Ibanez, V. Martinez, E. Roman and A. Sanz, “An innovative perturb, observe and check algorithm for partially shaded PV systems”, 2009 13th European Conference on Power Electronics and Applications, Barcelona, Spain, 06 October 2009, pp. 1-8.

[12] J. Archila Valderrama, M. Mantilla Villalobos, J. Barrero P´erez, J. Petit Suárez, and G. & Ordoñez Plata, “A maximum power point tracking algorithm for photovoltaic systems under partially shaded conditions”, Ingenieria Y Universidad, vol. 20, no. 2, pp. 391-410, 2016.

[13] Adedayo M. Farayola, Yanxia Sun and Ahmed Ali, “ANN-PSO Optimization of PV Systems Under Different Weather Conditions”, 7th International Conference on Renewable Energy Research and Applications, Paris, France, pp. 1363 - 1368, Oct. 14-17, 2018.

[14] Koray Şener Parlak and Hayrettin Can, “A new MPPT method for PV array system under partially shaded conditions”, 3rd IEEE International Symposium on Power Electronics for Distributed Generation Systems (PEDG), Aalborg, Denmark, pp. 437 - 441, 02 August 2012.

[15] Mohcine Mokhlis, Mohammed Ferfra, “Optimization of Photovoltaic Panels Efficiency Using a Backstepping Control Technique Under Partial Shading Conditions”, International Review on Modelling and Simulations (I.RE.MO.S), Vol. 10, No. 6, ISSN: 1974-9821, December 2017.

[16] Muralidhar Killi and Susovon Samanta, “Output voltage sensor based DMPPT with parallel configuration for PV systems under partial shading conditions”, 2016 IEEE Annual India Conference (INDICON), Bangalore, India, pp. 1-6, 02 February 2017.

[17] MRS.Sunita Ravi Kadali and Prof Mrs. V.S Jape, “A Distributed Maximum Power Point Control For Efficiency Enhancement Of Photovoltaic System”, International Journal of Innovative Research in Science,

Engineering and Technology, vol. 3, no. 3, ISSN: 2347-6710, 2014, pp. 179-183.

[18] Reza Rezaii, Mohammad Amin Abolhasani, Ali Yazdian Varjani, Reza Beiranvand, "New Strategy of Grid Connected Photovoltaic System Using Module Integrated Converters with B4 Inverter to Overcome Partial Shading Effect", 2015 30th International Power System Conference (PSC), Tehran, Iran, 23 January 2017.

[19] E. Duran, M. Sidrach-de-Cardona, J. Galan and J.M. Andujar, "Comparative Analysis of Buck-Boost Converters used to obtain I-V Characteristic Curves of Photovoltaic Modules", 2008 IEEE Power Electronics Specialists Conference, pp. 2036-2042, ISBN: 978-1-4244-1667-7, Rhodes, Greece, 08 August 2008.

[20] Moh. Zaenal Efendi, Farid Dwi Murdianto and Rangga Eka Setiawan, "Modeling and Simulation of MPPT Sepic Converter Using Modified PSO to Overcome Partial Shading Impact on DC Microgrid System", 2017 International Electronics Symposium on Engineering Technology and Applications (IES-ETA, pp. 27-32, Surabaya, Indonesia, 28 December 2017.

[21] Samet Biricik, Tuan Ngo, Hasan Komurcugil and Malabika Basu, "Nonlinear Control Methods for Single-Ended Primary-Inductor Power Converters", 43rd Annual Conference of the IEEE Industrial Electronics Society, Beijing, China, 18 December 2017.

[22] Mohcine Mokhlis, Mohammed Ferfra and Mohammed Chraygane, "Nonlinear Control of a Photovoltaic Pumping System under Partial Shading", 2017 International Renewable and Sustainable Energy Conference (IRSEC), pp. 1-7, ISSN: 2380-7393, Tangier, Morocco, 01 October 2018.

[23] Marcelo Gradella Villalva, Jonas Rafael Gazoli and Ernesto Ruppert Filho, "Comprehensive Approach to Modeling and Simulation of Photovoltaic Arrays", IEEE Transactıons on Power Electronics, Vol. 24, No. 5, MAY 2009, pp. 1198-1208

[24] Javier Cubas, Santiago Pindado and Marta Victoria, "On the analytical approach for modeling photovoltaic systems behavior", Journal of Power Sources, Vol. 247, pp. 467-4741, February 2014.

[25] Kai Chen, Shulin Tian, Yuhua Cheng and Libing Bai, "An Improved MPPT Controller for Photovoltaic System Under Partial Shading Condition", IEEE Transactions on Sustainable Energy,Vol. 5 , No 3, pp. 978-985, 2014.

[26] Vanxay Phimmasone, Yuta Kondo, Takayoshi Kamejima and Masafumi Miyatake, "Verification of Efficacy of the Improved PSO-based MPPT Controlling Multiple Photovoltaic Arrays", 2011 IEEE Ninth International Conference on Power Electronics and Drive Systems, Singapore, Singapore, pp. 1015-1019, 2011.

[27] Xiaorong Zhu, Shipeng Liu, Yuning Wang, Linlin Dou and Jie Cai, "A sliding mode control based maximum power point tracking method of PV arrays under partially shaded conditions", International Conference on Renewable Power Generation (RPG 2015), Beijing, China, pp. 1 – 5, 2015.